

- (33) Hunt, M. L.; Newman, S.; Scheraga, H. A.; Flory, P. J. *J. Phys. Chem.* **1956**, *60*, 1278.  
 (34) Huque, M. M.; Goring, D. A. I.; Mason, S. G. *Can. J. Chem.* **1958**, *36*, 952.

- (35) Motowoka, M.; Fujita, H.; Norisuye, T. *Polym. J.* **1978**, *10*, 331.  
 (36) Sadanobu, J.; Norisuye, T.; Fujita, H. *Polym. J.* **1981**, *13*, 75.  
 (37) Yamakawa, H.; Yoshizaki, T. *Macromolecules* **1980**, *13*, 633.  
 (38) Yoshizaki, T.; Yamakawa, H. *J. Chem. Phys.* **1980**, *72*, 57.

## Computer Simulation of the Dynamics of Star Molecules

R. J. Needs\* and S. F. Edwards

Cavendish Laboratory, Cambridge CB3 0HE, United Kingdom. Received December 16, 1982

**ABSTRACT:** A computer simulation of 3-branched star molecules is presented in both free and highly entangled regimes. The diffusion constant of the center of mass of an entangled chain is shown to be of the form  $D \propto N^{-b} \exp(-aN)$ , where  $N$  is the number of chain segments in an arm, while the free-chain data are in good agreement with the Rouse result  $D \propto N^{-1}$ . A relaxation time of the entangled molecule is shown to be of the form  $T \propto N^d \exp(cN)$  while the free-chain data agree with the Rouse result of  $T \propto N^2$ .

### Introduction

In a series of papers by Evans and Edwards<sup>1-3</sup> a computer simulation of free and entangled linear molecules was presented. The presence of the other polymers in the melt was represented by a mesh of infinitely long rods. They found that the diffusion constant of the center of mass,  $D$ , and the relaxation time,  $T$ , defined as the time when the end-to-end vector correlation  $\langle \mathbf{R}(t) \cdot \mathbf{R}(0) \rangle$  dropped to  $e^{-1}$  of its initial value obeyed

$$\begin{aligned} D &\propto N^{-2.0(\pm 0.2)} \\ T &\propto N^{3.1(\pm 0.2)} \end{aligned} \quad (1)$$

where  $N$  is the number of chain segments. This is in agreement with the reptation model of de Gennes.<sup>4</sup> In a later paper Evans<sup>5</sup> extended this work to 3-branched star molecules. For entangled stars he found

$$\begin{aligned} D &\propto N^{-3.0(\pm 0.2)} \\ T &\propto N^{3.9(\pm 0.2)} \end{aligned} \quad (2)$$

where  $N$  is the number of segments in an arm. de Gennes<sup>6</sup> has argued that, to diffuse, a 3-branched star molecule in a network of infinitely long, fixed obstacles would have to withdraw the end of one of its arms down its tube to the branching point and extend it, initially in the direction of another of the arms; see Figure 1. During the time scale of this process one could imagine the branching point as essentially fixed. He then calculated the probability of a configuration of an arm, with both ends coincident, in which the loop thus formed enclosed none of the obstacles, i.e., as in Figure 1b. He found that this probability  $P$  was given by

$$P(N) \propto \exp(-aN) \quad (3)$$

where  $a$  is a constant.<sup>6,7</sup> We have recalculated  $P$ , and for large  $N$  find

$$P(N) \cong \frac{2(2^{1/2})^z}{\pi^{1/2} N^{1.5}(z-1)} \exp(N \log(2(z-1)^{1/2}) - N \log(z)) \quad (4)$$

where  $z$  is the coordination number of the lattice.<sup>14</sup> As one of these retracing configurations must be intermediate to a diffusion or relaxation step, he argued that the diffusion constant would be proportional to this probability and the relaxation or renewal time to its inverse. Clearly this cannot be exact; different configurations should have different weights, but we have no way to calculate the weights and so assume them all equal.

It is important to note that the de Gennes mechanism is not the only possible one. If the branching point were to move  $p$  steps down the tube of one arm, dragging the other two arms behind it, one of these two arms which occupy  $p$  steps of the same tube would only have to disengage the remaining  $N-p$  steps for a diffusive step to occur. We can sum all the configurations intermediate to one of these diffusive steps to give a total probability  $M(N)$ .

$$M(N) = \sum_{p=0}^{N/2} P(2N-2p) \{1 - P(2p)\} \quad (5)$$

where we define  $P(0) = 0$ . The  $p = N/2$  term is the de Gennes mechanism.

Doi and Kuzuu<sup>8</sup> have used arguments based on the dynamics of an arm to calculate the same form for  $T$ . They then predict the forms of the creep compliance and viscosity of a melt of such stars, which are in good agreement with the data of Graessley and Roovers.<sup>9</sup>

### Model

The computer model is exactly that of Evans.<sup>5</sup> Only a brief description of the model is given here as a full description has already been published.<sup>1,5</sup> The polymer is modeled as a set of  $M$  points on a cubic lattice; the separation of neighboring points on the chain is one lattice spacing. No excluded volume interaction is used between points along the polymer. This ensures that the chain will have ideal chain statistics as is well-known to be the case in melts. A chain, linear or branched, is set up as a random walk on the lattice. Points along the chain are chosen at random and moved such that the chain remains connected and no portion of the chain has moved through any obstacles present. A time step is  $M$  such attempted moves. The obstacles are infinitely long rods located on a cubic lattice shifted from the polymer lattice in each of the Cartesian directions by  $1/2$  a lattice spacing. This set of obstacles is called the "cage". In this simulation obstacles were placed at each possible site; thus the distance between obstacles was the polymer step length. Previous simulations<sup>1-3,5</sup> used variable cage spacings, but as the molecule is most highly entangled with a cage spacing of 1, this spacing was used throughout.

As the model neglects both hydrodynamic and excluded volume interactions, it is not successful at modeling polymers in dilute solution. But if no obstacles are present and we model a free chain, we retrieve the results of the Rouse chain.<sup>11</sup> In particular, Evans found for both linear

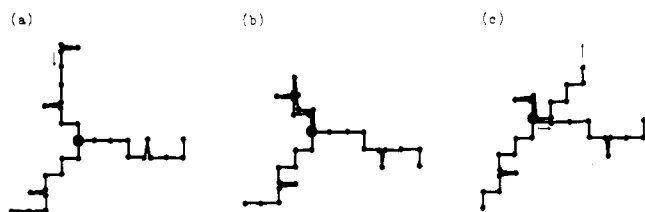


Figure 1. de Gennes mechanism of relaxation and diffusion, described in the text. The cage of obstacles is not shown.

and star molecules that the diffusion constant was inversely proportional to the number of chain segments and the longest relaxation time was proportional to the number of segments squared. Also at short times the average displacement squared of a monomer was proportional to  $t^{1/2}$ . It is also found that the coefficients of  $t^{1/2}$  for points at the end of a chain, the interior, and at a 3-fold branching point are in the proportions predicted by the Rouse theory:<sup>11</sup>

$$\langle (\mathbf{r}_n(t) - \mathbf{r}_n(0))^2 \rangle = (2D_{\text{mon}}/\gamma)t^{1/2} \quad (6)$$

where  $\gamma$  is the functionality of the branching point, i.e., 1 for an end point, 2 for an interior point of a linear chain, etc.

### Diffusion Constant

The diffusion constant of the center of mass is defined as

$$D = \lim_{t \rightarrow \infty} (1/t) \langle (\mathbf{R}_{\text{cm}}(t) - \mathbf{R}_{\text{cm}}(0))^2 \rangle \quad (7)$$

It is a property of the long time scale motion. If during the simulation the polymer was moved only a distance much smaller than the size of the molecule, we would measure an apparent diffusion constant that contained some of the short time scale motion and was thus larger than the real diffusion constant. The star molecule simulation of Evans<sup>5</sup> does not satisfy this criterion. For the longer entangled stars he did not have the computer time available to move the polymer far enough to measure the correct diffusion constant. For a chain with each arm 10 units long, in a cage spacing of 1, he could only move the center of mass an average distance squared of less than 3. Thus the diffusion constants he measured for highly entangled stars of large molecular weight are too big, while those for low molecular weight are accurate. He thus obtained a weaker dependence on the diffusion constant than is correct. In Figure 2 the apparent diffusion constant measured is plotted against the average distance squared the center of mass moved, for an entangled polymer of arm length 7, showing the apparent increase in  $D$  when the polymer is moved for short distances. In this simulation, for all measurements of  $D$  the average displacement squared of the center of mass was greater than the average end-to-end length squared of an arm.

In Figure 3,  $\log(D)$  is plotted against  $\log(N)$  for the free and entangled stars. A least-squares fit to the free-chain data gives

$$D = 0.42(\pm 0.02)N^{-0.92(\pm 0.05)} \quad (8)$$

The plot of  $\log(D)$  against  $\log(N)$  for the entangled chain is clearly curved, so that the relationship is not a simple power law. A least-squares fit to a function of the form

$$D = AN^{-B} \exp(-CN) \quad (9)$$

gives

$$\begin{aligned} A &= 0.033 \pm 0.004 \\ B &= 0.59 \pm 0.14 \\ C &= 0.37 \pm 0.02 \end{aligned} \quad (10)$$

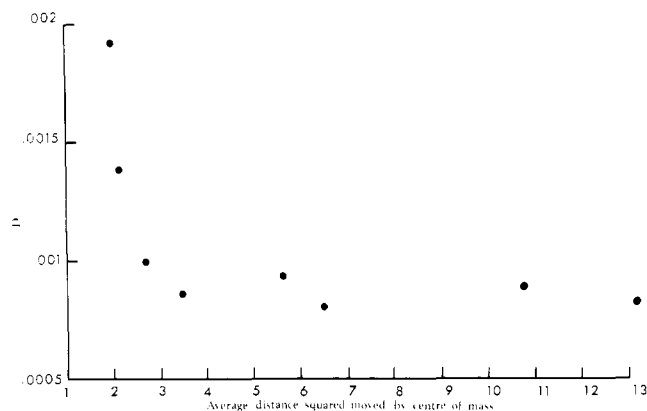


Figure 2. Plot of the apparent diffusion constant measured,  $D$ , against the average distance squared moved by the center of mass.

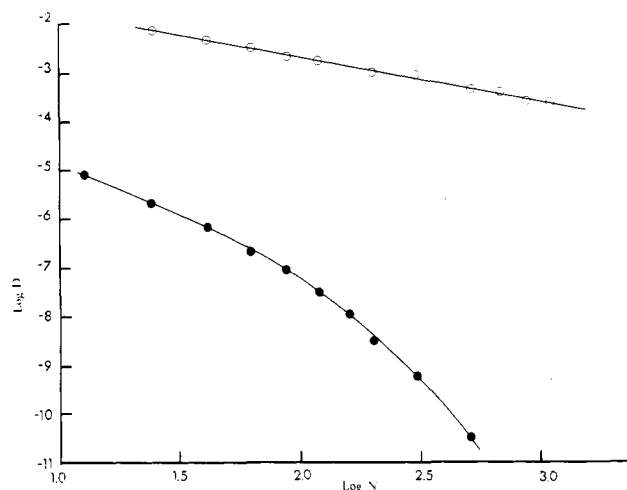


Figure 3.  $\log(D)$  against  $\log(N)$ : (O) free star; (●) entangled star. Regression lines indicated.

### Relaxation Time

The autocorrelation function of the vector  $\mathbf{R}$  from the end of one arm to the end of another is assumed to decay by a set of exponential modes

$$\langle \mathbf{R}(t) \cdot \mathbf{R}(0) \rangle = \langle \mathbf{R}(0)^2 \rangle \sum_n \exp(-t/T_n) \quad (11)$$

If we wait long enough, the longest relaxation time presumably dominates and we can write

$$\langle \mathbf{R}(t) \cdot \mathbf{R}(0) \rangle \cong \langle \mathbf{R}(0)^2 \rangle \exp(-t/T_{\text{max}}) \quad (12)$$

so that a plot of  $\log \langle \mathbf{R}(t) \cdot \mathbf{R}(0) \rangle$  against  $t$  has a gradient of  $-1/T_{\text{max}}$ . In this simulation we find that the relaxation modes of the entangled star are not separated well enough for this. So we define a relaxation time  $T$  by allowing the star to relax until  $\langle \mathbf{R}(t) \cdot \mathbf{R}(0) \rangle$  falls to  $e^{-1}$  of its initial value and fit the relaxation over this period to a single exponential (the fits of  $\log \langle \mathbf{R}(t) \cdot \mathbf{R}(0) \rangle$  against  $t$  have linear correlation coefficients of over 0.96). By this definition we have a relaxation time that still contains the essential information about relaxation time scales.

A plot of  $\log(T)$  against  $\log(N)$  is shown in Figure 4, for the free and entangled chains. A least-squares fit to the free-chain plot gives

$$T = 0.35(\pm 0.03)N^{1.94(\pm 0.04)} \quad (13)$$

The plot of  $\log(T)$  against  $\log(N)$  for the entangled chain is curved and a least-squares fit to

$$T = AN^B \exp(CN) \quad (14)$$

gives

$$\begin{aligned} A &= 2.4 \pm 0.4 \\ B &= 1.9 \pm 0.15 \\ C &= 0.195 \pm 0.015 \end{aligned} \quad (15)$$

The relaxation time was also measured when the branching point was forbidden to move; these results are also plotted in Figure 4.

### Discussion

The relaxation time and diffusion constant are found to vary exponentially with the arm length, but the exponents were found to be different. If the free star is allowed to relax for longer times so that  $\langle \mathbf{R}(t) \cdot \mathbf{R}(0) \rangle$  is  $e^{-1}$ ,  $e^{-2}$ ,  $e^{-3}$ , and  $e^{-4}$  of its initial value, the characteristic relaxation time measured is found to be almost constant, showing that we have measured the longest relaxation time of the free star, the Rouse time. When this was done for the entangled star, the characteristic time measured increased steadily as the star was allowed to relax for longer. This is because the relaxation modes of the entangled star are not well separated from one another. The star can relax a considerable way by bringing an arm part way down its tube and pushing it out in another direction. If the time to bring an arm end to the branching point is  $\exp(aN)$ , then modes  $\exp(a(N-1))$ ,  $\exp(a(N-2))$ , etc. also exist (see Figure 5), whereas for the entangled, reptating, linear chain the times are  $N^3/n^2$  for integer  $n$ . To relax so that  $\langle \mathbf{R}(t) \cdot \mathbf{R}(0) \rangle = e^{-1} \langle \mathbf{R}(0)^2 \rangle$  the arm must come a fraction  $1 - e^{-1} \cong 0.632$  of the way down its tube so that the relaxation time  $T$  as defined in this paper is related approximately to the longest relaxation time  $T_{\max}$  by

$$T(N) = T_{\max}(0.632N) \quad (16)$$

Thus if

$$T(N) \propto \exp(0.195N) \quad (17)$$

then

$$\begin{aligned} T_{\max}(N) &\propto \exp(0.195N/0.632) \\ &\propto \exp(0.31N) \end{aligned} \quad (18)$$

and we have much better agreement between the exponents for  $T_{\max}$  and  $D$ .

When the branching point was forbidden to move, the relaxation times measured were increased by a factor of between 1.2 and 1.8; see Figure 4. This indicates that motion of the branching point does not dominate the relaxation process.

### Conclusion

We have simulated a 3-branched star molecule by a model that, for a free chain, shows excellent agreement with the results for a Rouse chain. Entanglements were included as a regular array of infinite fixed obstacles in a model that, for linear molecules, has shown good agreement<sup>1</sup> with the theory of reptation.<sup>4</sup> We find that the diffusion constant of the entangled chains falls exponentially with increasing arm length as predicted by de Gennes.<sup>6</sup> A relaxation time of the molecule was measured and found to increase exponentially with arm length, which was also predicted by de Gennes.<sup>6</sup> The exponents measured for  $D$  and  $T$  are different. This is because the molecule must retract an arm to the branching point for a diffusive step but can relax so that the correlation of the end-to-end vector falls to  $e^{-1}$  of its initial value by retracting the arm only part way down its tube. Thus  $T$  is not the longest relaxation time of the entangled star but

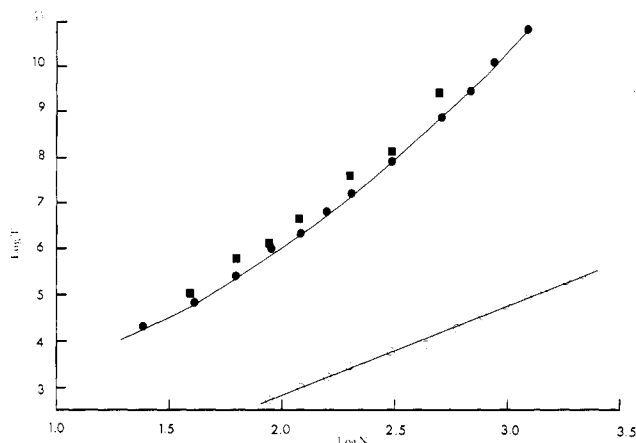


Figure 4.  $\log(T)$  against  $\log(N)$ : (○) free chain; (●) entangled star; (■) entangled star with branching point fixed. Regression lines are indicated.

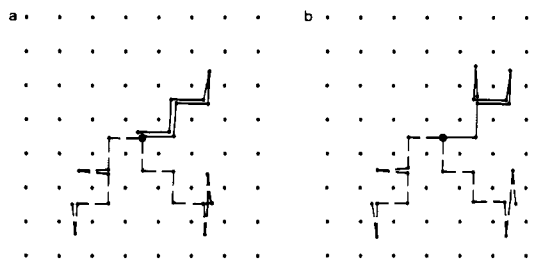


Figure 5. (a) Continuous line is an arm retracing itself to the branching point; relaxation mode of characteristic time  $\propto \exp(aN)$ . The dots represent obstacles. (b) Relaxation mode of characteristic time  $\propto \exp(a(N-2))$ .

is the longest relaxation time, the Rouse time for the free star.

For a cubic lattice,  $z = 6$ , eq 4 gives

$$P(N) \cong 1.915N^{-1.5} \exp(-0.294N) \quad (19)$$

and we have reasonable agreement between the exponents of  $P(N)$  and  $D$  and  $T_{\max}$ . We can evaluate the contribution from all mechanisms and evaluate  $M(N)$  over the simulation range  $N = 4-22$  and fit the values to a function of the form of  $P(N)$ . The fit is very good and we get

$$M(N) \cong 2.84N^{-1.06} \exp(-0.312N) \quad (20)$$

The mechanisms not included by de Gennes thus account for between 30% and 50% of  $M(N)$  in the simulation range.

The only cage spacing,  $a$ , used in this simulation was 1. If this was varied one would expect  $D$  and  $T$  to scale like  $N/a^2$ . One could also vary the number of branches,  $f$ , of the star. This would not be expected to alter  $T$  as in the relaxation process the arms are independent, but in the diffusion process the arms must behave cooperatively; in an  $f$ -armed star,  $f-2$  arm ends must be brought to the branching point for a diffusive step to occur, so that one expects  $T$  to scale like  $N/a^2$  for any  $f$  and  $D$  to scale like  $N(f-2)/a^2$ . As  $N$  is proportional to  $M/f$ , where  $M$  is the molecular weight, we note that for fixed  $M$  we could always construct a star, by making it with a sufficient number of arms, so that its diffusion constant was lower than that of a linear chain of molecular weight  $M$ , while the longest relaxation time of the star was also lower than that of the linear chain.

These results are for the motion of a star through a lattice of infinitely long obstacles. In melts of stars, tube rearrangement<sup>12,13</sup> might occur. For a star in a melt of linear chains one would expect tube rearrangement to

dominate the motion of the star for large molecular weights of the star.

**Note Added in Proof.** An  $f$ -armed star must bring  $f - 2$  arms to the branching point for a diffusive step. But the arm ends need not arrive at the branching point simultaneously so we might expect  $D$  to have a weaker  $f$  dependence than suggested in the text.

**Acknowledgment.** We thank Dr. J. Klein for useful discussions, especially as regards the diffusive mechanisms available to the entangled star. R.J.N. acknowledges the assistance of an SERC CASE award with ICI, Welwyn Garden City, U.K.

## References and Notes

- (1) Evans, K. E.; Edwards, S. F. *J. Chem. Soc., Faraday Trans. 2*, 1981, 77, 1891.
- (2) Edwards, S. F.; Evans, K. E. *J. Chem. Soc., Faraday Trans. 2*, 1981, 77, 1913.
- (3) Evans, K. E.; Edwards, S. F. *J. Chem. Soc., Faraday Trans. 2*, 1981, 77, 1929.
- (4) de Gennes, P. G. *J. Chem. Phys.* 1971, 55, 572.
- (5) Evans, K. E. *J. Chem. Soc., Faraday Trans. 2*, 1981, 77, 2385.
- (6) de Gennes, P. G. *J. Phys. (Paris)* 1975, 36, 1199.
- (7) de Gennes, P. G. "Scaling Concepts in Polymer Physics"; Cornell University Press: Ithaca, NY, 1979.
- (8) Doi, M.; Kuzuu, N. Y. *J. Polym. Sci., Polym. Lett. Ed.* 1980, 18, 775.
- (9) Graessley, W. W.; Roovers, J. *Macromolecules* 1979, 12, 959.
- (10) Rouse, P. E. *J. Chem. Phys.* 1953, 21, 1272.
- (11) Warner, M. *J. Phys. C, Solid State Phys.* 1981, 14, 4985.
- (12) Klein, J. *Macromolecules* 1978, 11, 852.
- (13) Daoud, M.; de Gennes, P. G. *J. Polym. Sci.* 1979, 17, 1971.
- (14) Another calculation of  $P(N)$  differing from eq 4 only in the preexponential factor has been reported: Helfand, E.; Pearson, D. S., to be published.

## Anisotropic Molecular Motion of Spin-Labeled Poly(methyl methacrylate) Detected by ESR

M. Shiotani and J. Sohma\*

Faculty of Engineering, Hokkaido University, Sapporo 060, Japan

J. H. Freed

Department of Chemistry, Cornell University, Ithaca, New York 14853.

Received February 1, 1983

**ABSTRACT:** Anisotropic rotational motion of the side chain in poly(methyl methacrylate) (PMMA) is inferred from the detailed analysis of the ESR spectrum of spin-labeled PMMA. Rotation about the axis parallel to the N-O bond of the nitroxide label bonded at the end of the ester side chains was twice as fast as that about the axes perpendicular to this bond in the incipient motional narrowing region. This axially symmetric rotation is discussed in terms of the molecular motions of PMMA.

## I. Introduction

It has been well established that both spin-probe and spin-label techniques are very useful to characterize molecular motions in synthetic polymers<sup>1</sup> as well as biopolymers.<sup>2</sup> ESR studies of molecular motion of spin-labeled polymers have two advantages: (1) easy detection of rapid motion on the time scale of nanoseconds to picoseconds and (2) selective detection of particular molecular motion of a part of the polymer, such as the end of a side chain that is labeled by a stable paramagnetic free radical. Poly(methyl methacrylate) (PMMA) is one of the polymers on which molecular motions have been studied by ESR combined with either the spin-labeling or the spin-probe method. For example, Miller and Veksli<sup>3,4</sup> reported ESR studies of spin-labeled PMMA, and Bullock and Cameron<sup>5</sup> and Shiotani and Sohma<sup>6,7</sup> also investigated the molecular motions of PMMA by ESR. These authors<sup>3-7</sup> have analyzed the observed spectra based on the assumption that the rotational reorientation was isotropic. Evaluation of the correlation time,  $\tau_R$ , of the rotational motion involved in spin-labeled PMMA relied upon the simplified expression of  $\tau_R$  proposed by Freed et al.<sup>8-11</sup> for isotropic rotation in the slow-motional region ( $10^{-9} \text{ s} \leq \tau_R \leq 10^{-6} \text{ s}$ ) and Kivelson's expression<sup>12</sup> for isotropic rotation in the motional narrowing region ( $10^{-11} \text{ s} \leq \tau_R \leq 10^{-9} \text{ s}$ ).

In previous studies,<sup>6,7</sup> the present authors also used these expressions as well as other simple expressions<sup>7,13</sup> for partial averaging to analyze the spectra. However, later investigation has shown that such an assumption is too simplified. There is no good reason to assume isotropic

motion for a labeling radical at the end of the ester chain of PMMA. It is more reasonable to allow for anisotropy in this particular molecular motion. In fact, Pilař et al.<sup>14a</sup> observed ESR spectra of the spin labels attached to the side chain of poly(methacrylamide)-type copolymers and concluded that the rotational reorientation was quite anisotropic and depended on the type of side chain. Freed and his collaborators<sup>11</sup> have developed an extensive theory of ESR spectra of nitroxides, which allows one to calculate the line shape for ESR spectra with a broad range of correlation times ( $10^{-12} \text{ s} \leq \tau_R \leq 10^{-6} \text{ s}$ ) and to treat various models of anisotropic rotational reorientation.

In this paper we report results obtained for spin-labeled PMMA with an analysis carried out in terms of the theory of Freed et al., and we compare these results with our earlier ones.

## II. Experimental Section

PMMA, which was spin labeled by a nitroxide radical at the end of the ester side chain, is the same sample used for the previous experiments.<sup>6,7</sup> One out of every 100 side chains was labeled by the nitroxide radicals. The details of the preparation of the polymer are described in the previous papers. A JEOL PE-X spectrometer was used with 100-kHz modulation, and the temperature control unit was used for temperature variation experiments.

## III. Analysis of ESR Line Shape

Temperature variations of the ESR spectra of the spin-labeled PMMA are shown in Figure 1. No change in the line shape was found at temperatures below 9 °C.